arXiv:1501.00598v1 [astro-ph.SR] 3 Jan 2015

Computer Simulation of Convective Plasma Cells

Rodrigo Carboni and Francisco Frutos-Alfaro
Space Research Center (CINESPA) and School of Physics
University of Costa Rica, San José, Costa Rica
Emails: rcarboni@cariari.ucr.ac.cr, frutos@fisica.ucr.ac.cr

January 6, 2015

Abstract

Computer simulations of plasmas are relevant nowadays, because it helps us understand physical processes taking place in the sun and other stellar objects. We developed a program called `PCell` which is intended for displaying the evolution of the magnetic field in a 2D convective plasma cell with perfect conducting walls for different stationary plasma velocity fields. Applications of this program are presented. This software works interactively with the mouse and the users can create their own movies in `MPEG` format. The programs were written in `Fortran` and `C`. There are two versions of the program (`GNUPLOT` and `OpenGL`). `GNUPLOT` and `OpenGL` are used to display the simulation.

1 Introduction

The huge advance in computer technology makes it possible to simulate and visualize complex physical phenomena taking place in stellar objects, *e.g.*, the convective plasma cells on the sun.
To understand the dynamo mechanism, most researchers consider cosmic plasma with a stationary motion, which leads to an induction problem. The aim is to find stationary states as solutions of the induction equation. Elsasser [5], Weiss [13] and Parker [10] performed the first two-dimensional simulations using symmetric velocity fields.

Simulations by Weiss and Galloway include dynamical effects and are generalized to three dimensions for the kinetic case (Weiss [13], Galloway *et al.* [7], Galloway and Weiss [8]). In recent years, dynamo models have been improved by considering fully dynamical solutions of the induction equation taking into account the coupled mass, momentum and energy relations for the plasma. Recently, Mininni et al. [9] have considered the Hall current into the dynamo model.

We can simulate convection cells by choosing convective velocity fields, which in turn help us understand the behavior of granules, mesogranules in the photosphere, supergranules in the photosphere and chromosphere, and laboratory plasmas. We also can investigate the not-well-understood phenomena of reconnection in this way [1].

The `PCell` program [2] helps visualize the magnetic field evolution in different convective plasmas. This program runs on `Linux` or `Unix`. The program can be downloaded from

`http://cinespa.ucr.ac.cr/software/xpcell/`

The capability to easily create movies in `MPEG` format is one of the main features of `PCell`.

2 The Induction Equation

Maxwell's Equations determine electromagnetic fields behavior in a cosmic fluid

$$\epsilon \nabla \cdot \mathbf{E} = \rho \tag{1}$$

$$\nabla \times \mathbf{E} = -\frac{\partial \mathbf{B}}{\partial t}, \tag{2}$$

$$\nabla \cdot \mathbf{B} = 0, \tag{3}$$

$$\nabla \times \mathbf{B} = \mu \mathbf{J} + \mu \epsilon \frac{\partial \mathbf{E}}{\partial t}, \tag{4}$$

where ρ is the charged particles density. The effects produced by the temperature gradient and charged particles density fluctuations had been neglected. The general expression for the current density $\mathbf{J}$ in an isotropic homogeneous medium is:

$$\mathbf{J} = \sigma \mathbf{E} + \sigma \mathbf{v} \times \mathbf{B} + \rho \mathbf{v} \tag{5}$$

where the right-hand-side terms are the conduction, induction and convection currents respectively. The conductivity σ is considered constant in the whole plasma and $\mathbf{v}$ is the velocity field that describes the plasma motion.
We can simplify the above equations by comparing the orders of magnitude of the quantities involved. We represent orders of magnitude with square brackets.
In cosmic plasmas the velocity of the charged particles (mechanical velocities) are much slower the electromagnetic field velocity (speed of light). Therefore, we have:

$$\left[\frac{v}{c}\right] = [\beta] \ll 1, \tag{6}$$

which implies that the orders higher than β can be neglected (non relativistic plasma).
From the Faraday equation (the second equation of 1), we can obtain an quantity with dimensions of velocity:

$$[E] = [v_{el}B], \tag{7}$$

which is the velocity associated to the electromagnetic processes and satisfies the condition:

$$[v_{el}] \leq [v]. \tag{8}$$

The last two equations combined give us an estimation of the rate of the electric energy to the magnetic energy:

$$\left[\frac{\epsilon E^2}{\mu^{-1}B^2}\right] = \left[\frac{E^2}{c^2B^2}\right] \leq [\beta^2]. \tag{9}$$

If equation (8) is fullfil, the electric component $\rho\mathbf{E}$ of the magnetic force that exerts the magnetic field over the plasma is negligible compared with the magnetic component $\mathbf{J} \times \mathbf{B}$.
The displacement current in the Ampere-Maxwell equation (the last equation of 1) is negligible when is compared to the conduction current. The rate of both is given by γ:

$$\gamma = \left[\frac{\omega_{el}\epsilon}{\sigma}\right], \tag{10}$$

where ω_{el} is the electromagnetic frequency. Taking L as a characteristic length of the electromagnetic and mechanical phenomena [5], we have

$$[v] = [L\omega], \tag{11}$$

and from (10) we obtain

$$[\omega_{el}] \leq [\omega]. \tag{12}$$

For the Earth's core $\gamma \leq 10^{-18}$ and for stars $\gamma \ll 1$ [4].
The rate of the convection current to the conduction current has the same value γ. From the Gauss law for the electric field (first equation of 1) we have that $[\rho] = [\epsilon E/L]$, therefore

$$\left[\frac{\rho v}{\sigma E}\right] = \left[\frac{\epsilon v}{\sigma L}\right] = [\gamma]. \tag{13}$$

According to equations (10) and (13), equation (5) and the last equation of (1) simplify to

$$\mathbf{J} = \sigma\mathbf{E} + \sigma\mathbf{v} \times \mathbf{B}, \tag{14}$$

and

$$\nabla \times \mathbf{B} = \mu\mathbf{J}. \tag{15}$$

respectively.
Combining the latter two equations we obtain

$$\nabla \times \mathbf{B} = \mu\mathbf{J} = \mu\sigma\mathbf{E} + \mu\sigma\mathbf{v} \times \mathbf{B}. \tag{16}$$

To eliminate $\mathbf{E}$, we apply the curl to equation (16) and make the substitution of Faraday's law (1), yielding

$$\mu\sigma\frac{\partial \mathbf{B}}{\partial t} = \mu\sigma\nabla \times (\mathbf{v} \times \mathbf{B}) - \nabla \times \nabla \times \mathbf{B}. \tag{17}$$

Finally, if we change the second term of the right side with the help of the well known identity and use the magnetic Gauss law (third equation of 1) we arrive to the induction equation

$$\frac{\partial \mathbf{B}}{\partial t} = \nabla \times (\mathbf{v} \times \mathbf{B}) + \eta\nabla^2\mathbf{B}, \tag{18}$$

where $\eta = 1/\mu\sigma$ is the magnetic viscosity.

3 Behavior of the Induction Equation

The rate of the first term on the right side of the induction equation to the second one is given by $R_m = Lv/\eta$, where the adimensional quantity is called the magnetic Reynolds number, in analogy to the Reynolds number for non conducting fluids. The bigger the plasma characteristic lengths is, the bigger the magnetic Reynolds number.
If the first term is much bigger than the second, equation (18) can be written as

$$\frac{\partial \mathbf{B}}{\partial t} = \eta \nabla^2 \mathbf{B}. \tag{19}$$

This is the diffusion equation, which describes the magnetic field decay in a diffusion characteristic time

$$\tau_\eta = \frac{L^2}{4\pi^2 \eta} \tag{20}$$

for a plasma with spherical symmetry. It is of the order of one second for a one centimeter radii copper sphere, 10^4 years for the Earth's nucleus and 10^{10} years for the Sun.
The order of the magnetic Reynolds number can be written as

$$[R_m] = \left[\frac{\omega}{\omega_{el}}\right] = \left[\frac{\tau_\eta}{\tau_0}\right] \tag{21}$$

where τ_0 is the time associated to plasma mechanical motion. Therefore, for times much slower than the diffusion time the equation simplifies to

$$\frac{\partial \mathbf{B}}{\partial t} = \nabla \times (\mathbf{v} \times \mathbf{B}) \tag{22}$$

which states that the magnetic flux trough any closed curve that moves with the local velocity of the plasma remains constant in time, i.e., the magnetic field lines are dragged by the fluid (*frozen field lines*).
When $R_m \gg 1$ the transport of the field lines by the plasma dominates over the diffusion, but if $R_m \ll 1$ the field decays very fast and the dynamo effect cannot take place. The behavior generated from the interplay of both terms for magnetic Reynolds number values between these limits is very interesting and to explore it is the aim of this work.

4 The Vector Potential Function

The induction equation (18) can be simplified for the two dimensional case if it is written as a function of the vector potential. We take the magnetic field and the velocity field limited to the $x-y$ plane, then the magnetic field is obtained from the one component vector potential $\mathbf{A} = A\mathbf{k}$ as follows

$$\mathbf{B} = \nabla \times \mathbf{A} = \left(\frac{\partial A}{\partial y}, -\frac{\partial A}{\partial x}, 0 \right), \tag{23}$$

after the substitution, equation (18) yields

$$\frac{\partial A}{\partial t} = -\mathbf{u} \cdot \nabla A + \eta \nabla^2 A. \tag{24}$$

We define the position and velocity variables as function of the characteristic parameters (maximum velocity U and maximum length L) as follows

$$u = u'U, \qquad x = x'L \tag{25}$$

with the analogous definition for the y coordinate. The spatial derivatives are given by

$$\frac{\partial}{\partial x} = \frac{1}{L}\frac{\partial}{\partial x'} \tag{26}$$

and

$$\frac{\partial^2}{\partial x^2} = \frac{1}{L^2}\frac{\partial^2}{\partial x'^2}. \tag{27}$$

After the substitution of these relations and defining a the characteristic time of the mechanical motion $\tau_0 = L/U$. For instance, if we take following velocity values for granules, mesogranules and supergranules in the sun,
$V = 900$, 60 and 400 m/s and $L = 1.4 \times 10^3$, 7×10^3 and 3×10^5 km, respectively, yield $\tau_0 = 26$ min, 1.35 and 0.87 days (Foukal [6], Sturrock *et al.* [11]). This time τ_0 measures the time it takes the plasma to go from the bottom to the top of the cell. With $t = t'\tau$, we obtain

$$\frac{\partial A}{\partial t} = \mathbf{u} \cdot \nabla A + \frac{1}{R_m}\nabla^2 A, \tag{28}$$

where the primes have been removed for clarity.
This is the equation we solve under the kinematic condition, i.e., there is no reaction of the magnetic field on the plasma, leaving the velocity field time

independent. This approach is valid if the magnetic energy is small compared with the kinetic energy of the plasma, that is

$$\frac{B^2}{8\pi\mu} \ll \frac{1}{2}\rho v^2. \tag{29}$$

5 The Visualization Program

5.1 Description of the Program

Equation (28) is solved using a fourth order difference schema in a two dimensional cell with perfect conducting upper and lower walls (the magnetic field lines remain always tide to them) and periodic conditions at the lateral walls, i. e., each cell is surrounded by similar cells.
The velocity field is taken to be incompressible, which allow us to define a stream function from which it can be obtained. we chose the following stream function [13] (see Figure 2)

$$\begin{aligned} \psi &= -\frac{1}{4\pi}\left(4(1-m)\left(x-\frac{1}{2}\right)^2 - m\right) \\ &\times \left(1-4\left(y-\frac{1}{2}\right)^2\right)^4 \cos\pi\left(x-\frac{1}{2}\right) \end{aligned} \tag{30}$$

with ($0 \le x \le 1$, $0 \le y \le 1$), m is an adjustable parameter ($0 \le m \le 1$) that allow us to select different velocity fields.
When $m = 1$ it describe a single eddy [13], as m decreases two new symmetrical eddies emerge from each side compressing the original eddie, at one time there are three eddies and as m get closer to zero, the central eddie disappear and remain just two eddies rotating in opposite directions.

5.2 The Visualization Program

The program called `pcell` is compressed in the `pcell.tar.gz` file. The program was originally written in `Fortran`. We translated them into `C` with the help of `F2C`. The `XFORMS` library, which is used to design the control panel is also required. The data generated by the program is processed by `GNUPLOT` (`PCell`) or `OpenGL` (`XPCell`) to produce the simulation.

When the program starts, it creates a window: the *PCell Control Panel*. The user can control all items on it by clicking.

5.3 The Control Panel

The parameters are adjusted interactively by the user with the mouse. The control panel has the following items (see Figure 1):

- The velocity field parameter selector: The user chooses the velocity field selecting a value of the m parameter, $(0 \leq m \leq 1)$.
- The magnetic Reynolds number selector: The user selects the magnetic Reynolds number, $(0 < R_m \leq 1000)$. The values of U and L are chosen equal to one.
- The time window: Displays the running time in units of $\tau_0 = L/U$.
- The maximum running time selector: The time at which the program stops running can be chosen with this button.

  This items can be selected in any order but they should be selected before any other item of the program.
- The Draw button: This button starts the program that calculates the magnetic field at each time interval (these data is stored in the files `pcell1.dat`, `pcell2.dat` and so on) and after a short time, when the generation of data is finished, the display window opens (see Figure 3).
- The display window: The evolution of the magnetic field lines are displayed in this window. When a given velocity field is selected it is shown here too.
- The Stream button: Displays the mechanical motion of plasma (see Figure 2).
- The Movie button: The users can create their own movies and with `XANIM` or a `MPEG` player they can display the movies. The name of the created movie is `convection.mpg`.
- The Help button: Gives the user a program guide.
- The Exit button: To leave the session. If the user wants to remove all `pcell*.dat` then type `rm -rf pcell*.dat` on the prompt.

6 Applications

There are some interesting applications that the user can explore. Among these are:

- The evolution of the magnetic field lines as function of the magnetic Reynolds number.
- The mechanism of magnetic field dissipation and the reconnection phenomena.
- The evolution of the averaged magnetic density as function of the magnetic Reynolds number.
- The maximum averaged magnetic density as function of the magnetic Reynolds number.
- The stationary state of the averaged magnetic density and the way it is reached as function of the magnetic Reynolds number.
- The time it takes to reach the maximum and the stationary state of the averaged magnetic density as function of the magnetic Reynolds number.

6.1 Evolution of the magnetic field

The stream function and the magnetic field twist evolution can be visualized easily with PCell. In Figure 2, an illustration of this evolution can be seen. Reconnection of the magnetic field appears in Figure 2b.

6.2 Analysis of the magnetic field evolution

For high Reynolds numbers, the convection generates a magnetic field component parallel to the plasma motion. The field begins to amplify itself, becoming stronger at the lateral borders of the cell (see Fig. 3). As this happens the spatial scale, where the variation of the field occurs, decreases linearly producing an increase of the diffusion. When this resistive term becomes of the same order as the convective term, the amplification of the field stops. Therefore, the averaged magnetic density reaches a maximum (see

Figure 4). The twisting of the field produces regions of high magnetic density at the same time that the diffusive term becomes bigger and reconnection of the magnetic filed lines occur expelling the field from the central region of the eddy reaching the magnetic density a stationary value (see Figure 2f). This stationary value is independent of the velocity field, but the way it is reached depends on the velocity field (see Figure 4).
For velocity fields dominated by one eddy, the magnetic energy in the central part of the cell is very small compared with the density at the borders. As the field is expelled from the central part by diffusion, the magnetic density does not change much so the stationary value comes from the field located at the borders. For velocity fields with a strong influence of lateral eddies an additional region of high magnetic density appears in the middle of the cell, where the central eddy is located (see Fig. 3a - d). The intensity of the field is of the same order as the one at the borders; the twisting of the field as it disappears on both sides of the central region of high density makes the average magnetic density oscillate until it reaches the stationary value. When the velocity fields are practically two eddies (small m), the magnetic field at the borders is not very strong and the generation of the central high density zone helps to reach the maximum value which is the same as the stationary one (see Figure 4).
It is important that the average lifetime of the granules and mesogranules is very small compared to the characteristic time (~ 0.31 and $0.07\tau_0$, respectively). Therefore for these motions, the behavior shown would not evolve because the structures have disappeared long before. On the other hand, in supergranules ($\sim 23\tau_0$) the stationary state is reached.
According to the above description for single eddies, a simple expression for the maximum averaged energy density and the Reynolds number can be obtained as $B^2_{max} \simeq R^{2/3}B^2$, where B_0 is the initial averaged magnetic field (Weiss [13], Carboni [1]). In Figure 5a, it can be seen that this behavior is still valid for plasmas with interacting eddies. The Reynolds number exponents obtained for the values of $m = 1.0$, 0.7, 0.3 and 0.1 are, respectively, 0.59, 0.55, 0.54 and 0.67. In the same way, a relation between the stationary and averaged energy density is obtained (Weiss [13], Carboni [1]) as $B^2_{st} \simeq R^{1/2}B^2$. Figure 5b shows the result of the simulations which agree very well with this relation even for interacting eddies. The Reynolds number exponents obtained in this case are 0.42, 0.42, 0.43 and 0.48 in the same order as above.

7 Conclusions and Future Work

The kinematical dynamo model presented here produces intensification of the magnetic field by the induction of plasma trying to move across field lines in regions of small eddies between big convective zones in addition to the usual one accumulated on the regions between cells. Although this model does not include the feedback of the $\mathbf{J} \times \mathbf{B}$ force on the inducting motion and has no rotation profile, the generation of a toroidal field is clear. Similar oscillatory behavior of the magnetic field for bands of asymmetrical eddies has been found for groups of four-cell convections by Zegeling [15] working on the same principle described here.
The model could be implemented to solve the full dynamo problem, which involves the simultaneous solution of the induction equation along with the equations of motion, continuity and thermodynamics. The inclusion of the $\mathbf{J} \times \mathbf{B}$ term produces freezing of the magnetic field to the electron flow instead of the bulk velocity field (Mininni *et al.* [9]).
Implementations of the numerical methods will allow us to expand the study, including the effects of nonlinearity and chaotic motion at Reynolds numbers typical of astrophysical problems where self-organization emerges (Chang *et al.* [3], Valdivia et al. [12]). New approaches have been developed to calculate, in a more efficient way, convective cells. One strategy is the adaptive grid method which, based on coordinate transformations between physical and computational coordinates, automatically tracks and spatially resolves nonlinear structures (Zegeling and Keppens [16]).

Future Work. The program can be improved in the following way:

- Including more velocity fields.
- Adding the magnetic density averaged over the cell, represented as function of time.
- Expanding to three dimensional cells and using other shapes like hexagonal cells (this shape appears as stable patterns in some fluids).
- Considering mechanical-electromagnetic interaction between the plasma and the field.
- Exploring more complex behaviors such as Chaos.
- Using the more advance program `XANIM` to produce a better animation.

8 Acknowledgment

The authors would like to thank Dr. Jorge Páez for his helpful comments.

References

[1] R. Carboni, *Convective Plasmas*, M. Sc. Thesis, School of Physics, University of Costa Rica, 1994.

[2] R. Carboni, and F. Frutos-Alfaro, *PCell: A 2D Program for Visualizing Convective Plasma Cells*, Computing in Science and Engineering, 2 - 5, July/August, 2004.

[3] T. Chang, S. W. Y. Tam and C. Wu, *Complexity induced anisotropic bimodal intermittent turbulence in space plasmas*, Physics of Plasmas, 11, 1287 - 1299, 2004.

[4] A. Z. Dolginov, *Magnetic field generation in celestial bodies*, Physics Reports 162: 337 - 415, 1988.

[5] W. M. Elsasser, *Hydromagnetic Dynamo Theory*, Reviews of Modern Physics, 28, 135 - 163, 1956.

[6] P. Foukal, *Solar Astrophysics*, Wiley & Sons, New York, 1990.

[7] P. A. Galloway, M. R. E. Proctor and N. O. Weiss, *Magnetic flux ropes and convection*, Journal of Fluid Mechanichs, 87, 243 - 254, 1978.

[8] P. A. Galloway, and N. O. Weiss, *Convection and Magnetic Fields in Stars*, Astrophysical Journal, 243, 120 - 130, 1981.

[9] P. D. Mininni, D. O. Gomez, and S. M. Mahajan, *Dynamo Action in Magnetohydrodynamics and Hall-Magnetohydrodynamics*, Astrophysical Journal, 587, 472 - 481, 2003.

[10] E. N. Parker, *Kinematical hydromagnetic theory and its applications to the low solar photosphere*, Astrophysical Journal, 138, 552 - 562, 1975.

[11] P. A. Sturrock, T. Holzer, D. M. Mihalas, D. M., R. K. Ulrich, (Editors), *Physics of the Sun*, Reidel, Dordrecht, 1986.

[12] J. A. Valdivia, A. Klimas, D. Vassiliadis, V. Uritsky and J. Takalo, *Self-organization in a current sheet model*, Space Science Reviews, 107, 515 - 522, 2003.

[13] N. O. Weiss, *The Expulsion of Magnetic Flux by Eddies*, Proceedings of the Royal Society, 293, 310 - 328, 1966.

[14] N. O. Weiss, *Magnetic Fields and Convection*, Advanced Chemical Physics, 32, 101 - 110, 1975.

[15] P. A. Zegeling, *On resistive MHD models with adaptive moving meshes*, Journal of Scientific Computing, Special ICIAM issue, 2005.

[16] P. A. Zegeling and R. Keppens, in *Adaptive Method of Lines* by A. Vande Wouwer, Ph. Saucez, and W. E. Schiesser (Editors), Chapman & Hall/CRC, 2001.

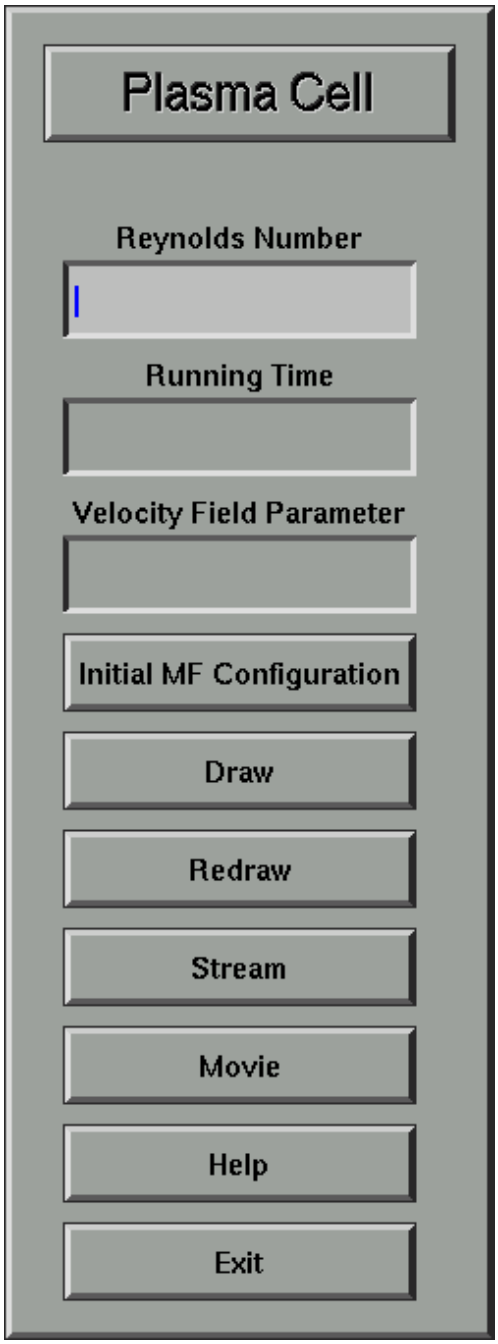

Figure 1: PCell Control Panel

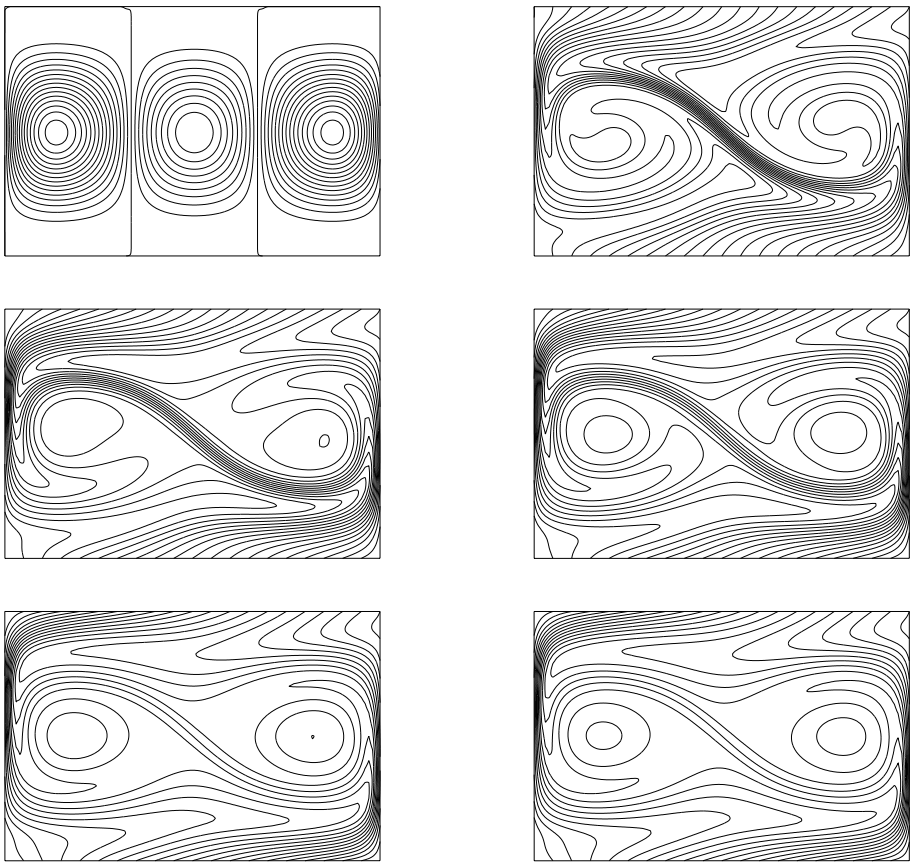

Figure 2: The stream function for $m = 0.1$ (a) and the corresponding time evolution of the magnetic field with $R_M = 1000$ (b-f) at times $t = 1$, 1.5, 2, 2.5, 3.

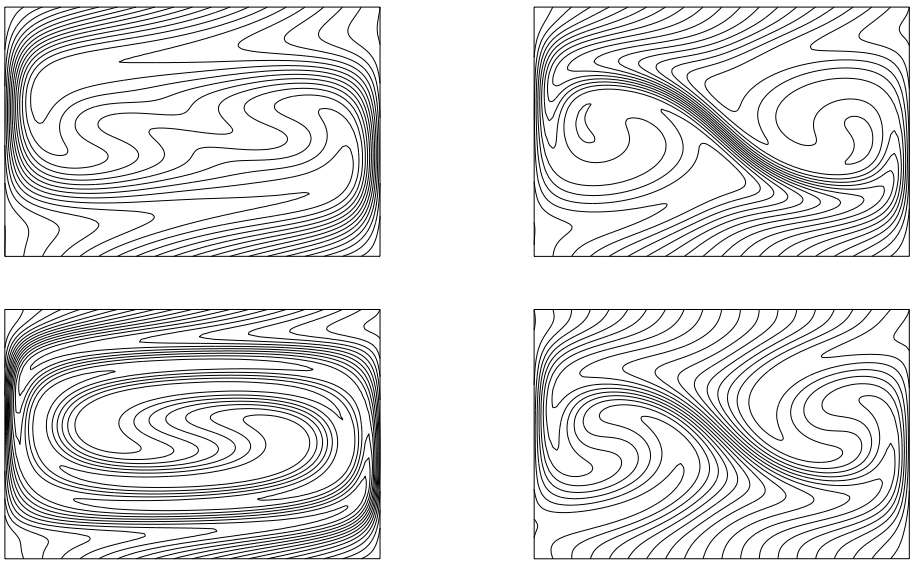

Figure 3: Magnetic field states for different magnetic Reynolds numbers and plasma velocity fields: (a) $R_m = 200$, $m = 0.1$, (b) $R_m = 500$, $m = 0.3$, (c) $R_m = 800$, $m = 0.7$ and (d) $R_m = 1000$, $m = 0.1$.

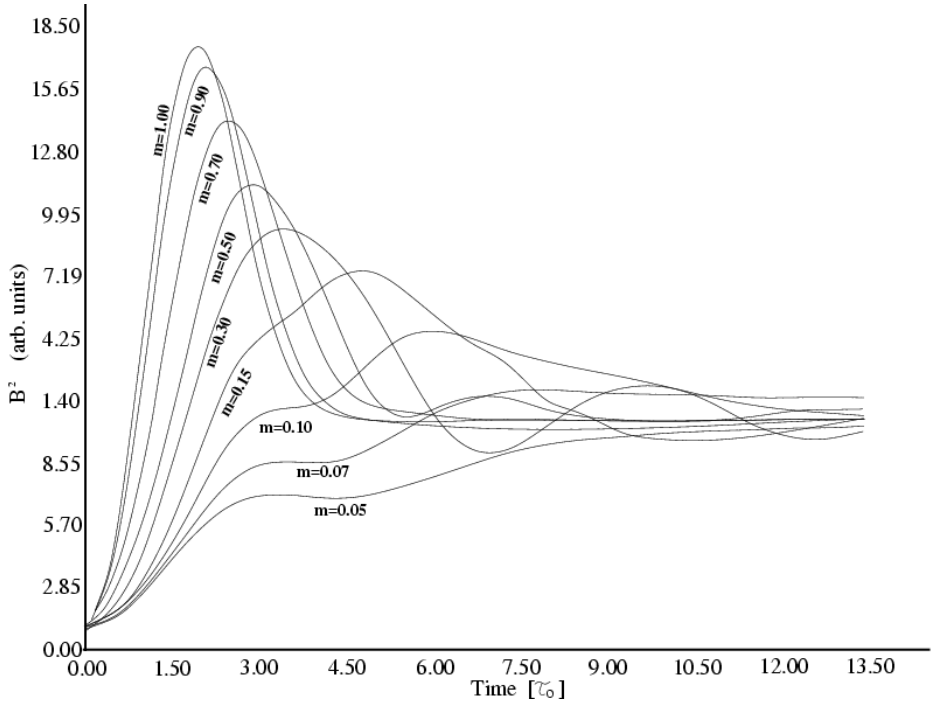

Figure 4: Square of magnetic field as a function of time for different m values.

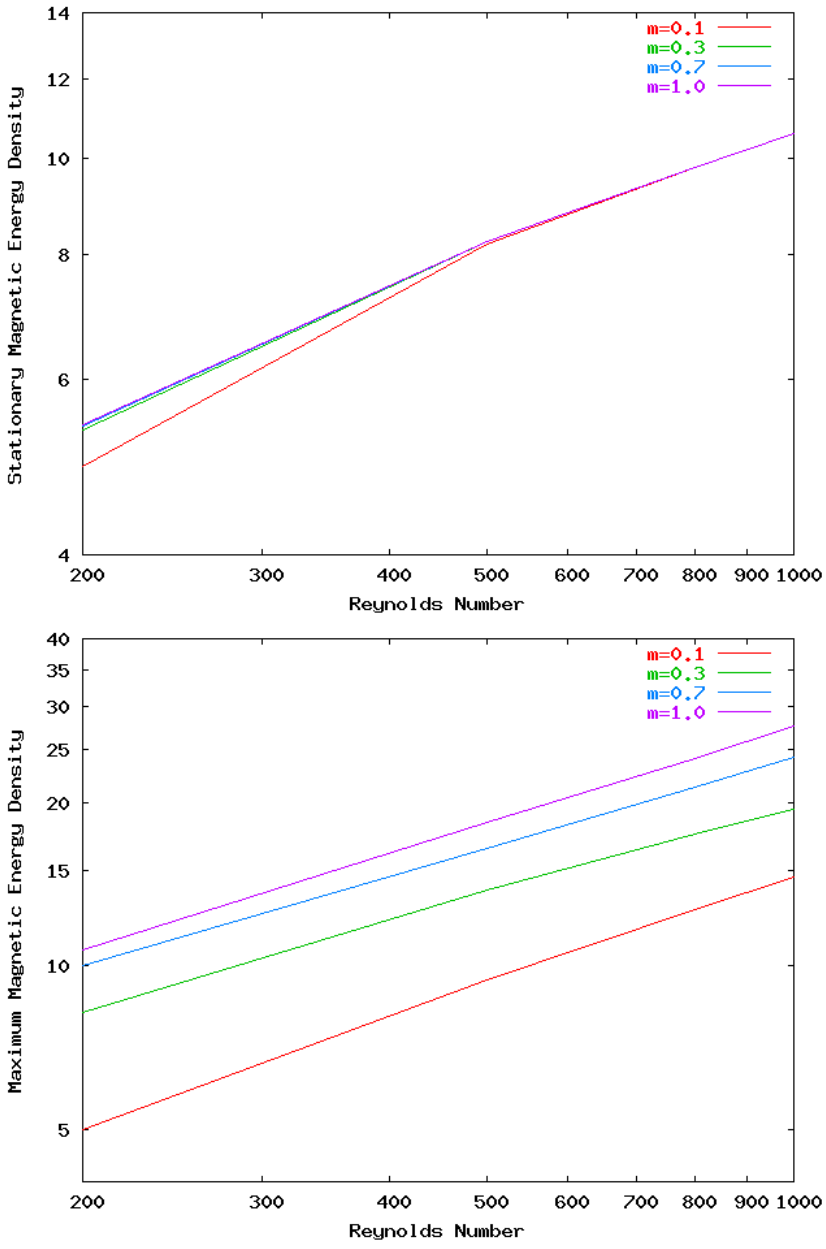

Figure 5: Stationary (a) and maximum magnetic energy density (b) as function of the magnetic Reynolds number for different m values.